INTERNATIONAL JOURNAL FOR NUMERICAL METHODS IN FLUIDS, VOL. 4, 1149–1163 (1984)

# PRESSURE AND TIME TREATMENT FOR CHEBYSHEV SPECTRAL SOLUTION OF A STOKES PROBLEM

M. DEVILLE*

*Université Catholique de Louvain, Unité de Mécanique Appliquée, 1348 Louvain-La-Neuve, Belgium*

L. KLEISER

*DFVLR, Institut für Theoretische Strömungsmechanik, 3400 Göttingen Federal Republic of Germany*

AND

F. MONTIGNY-RANNOU†

*Office National d'Etudes et de Recherches Aérospatiales (O.N.E.R.A.). 92320 Châtillon, France*

## SUMMARY

To investigate the influences of time scheme, pressure treatment and initial conditions in incompressible fluid dynamics, a Stokes problem is solved numerically on a slab geometry within the framework of spectral approximation in space. Four algorithms are examined: splitting schemes, influence matrix method, penalty formulation and pseudo-spectral space–time technique. It is shown that splitting schemes are less accurate than the other processes. Furthermore, the initial field should respect a compatibility condition to avoid singularities at the initial time. If it is not possible to build such a compatible field, the numerical procedure has to present good damping properties at the first steps of the time integration.

KEY WORDS Stokes Problem Chebyshev Approximation Spectral Method Penalty Formulation Splitting Scheme

## 1. INTRODUCTION

The numerical solution of incompressible viscous flows calls for special treatment of pressure and continuity equation with the velocity–pressure formulation of the basic equations. Our aim is to investigate the influences of time scheme, pressure treatment and initial conditions on the numerical solution of the two-dimensional Stokes problem within the context of spectral approximation in space, namely Chebyshev polynomials in the $x$ direction and periodic Fourier series in the $y$ direction. Several algorithms are used for the time integration and the pressure computation.

Owing to the excellent accuracy of spectral methods, calculations carried out by large fluid dynamics codes such as CHANSON[1] bring up the problem of pressure calculation. Therefore, the Stokes problem constitutes a model which contains all the characteristic features of the Navier–Stokes equations from the point of view of pressure determination.

---

*Also collaborator of the Office National d'Etudes et de Recherches Aérospatiales, 92320 Châtillon, France.

†Correspondence should be sent to F. Montigny-Rannou, O.N.E.R.A., B.P. 72, 92322 Châtillon Cédex, France

0271–2091/84/12 1149–15$01.50

*Received 29 June 1983*
*Revised 9 January 1984*

Section 2 states the Stokes problem, which was previously considered as a test problem at a GAMM workshop held in Louvain-la-Neuve in October 1980. As the Stokes problem is linear, an analytical solution may be obtained and it is therefore possible to compare the computed decay-rate of the solution to the exact value. In Section 3, the various numerical schemes are described. They include the splitting method, the influence matrix technique which imposes a vanishing boundary divergence, the penalty formulation and finally the pseudo-spectral space–time algorithm. Section 4 introduces two initial velocity fields. The first one, although incompressible, does not satisfy the compatibility condition. The second velocity field ensures that the incompressibility constraint is satisfied with an initial pressure field verifying both Neumann and Dirichlet conditions. In Section 5, the numerical results are presented.

The present analysis shows that the initial and boundary conditions of a mixed (initial and boundary value) problem must be compatible in order to avoid singularities at the initial time and development of spurious numerical oscillations. If a compatible initial field cannot be found, the numerical process must possess good damping properties to cope with the initial singularities during the first steps of the time integration.

## 2. PROBLEM STATEMENT

Consider the two-dimensional Stokes problem defined on the infinite slab in the $y$ direction with $|x| \leqslant 1$. The equations are

$$\frac{\partial \mathbf{v}}{\partial t} = -\,\mathbf{grad}\, p + \nu \Delta \mathbf{v} \tag{1}$$

$$\operatorname{div} \mathbf{v} = 0. \tag{2}$$

In equations (1) and (2), $\mathbf{v}$ is the velocity field, $p$ the pressure and $\nu$ the kinematic viscosity. The linear problem is subject to the boundary conditions $\mathbf{v} = 0$ at $x = \pm 1$ and to an initial condition: $\mathbf{v}(\mathbf{x}, t = 0)$. Let us assume periodicity in the $y$ direction, such that the solution of equations (1) and (2) may be decomposed into Fourier modes:

$$\mathbf{v}(\mathbf{x}, t) = \sum_{-K}^{K} \bar{\mathbf{v}}(x, t) \mathrm{e}^{jky},\ p(\mathbf{x}, t) = \sum_{-K}^{K} \bar{p}(x, t) \mathrm{e}^{jky}$$

$K$ being the cut-off of the Fourier series.

As the complete solution can be obtained by linear superposition, we will restrict our attention to a particular mode in such a way that we define

$$\mathbf{v}(\mathbf{x}, t) = \bar{\mathbf{v}}(x, t) \mathrm{e}^{jky},\ p(\mathbf{x}, t) = \bar{p}(x, t) \mathrm{e}^{jky} \tag{3}$$

By insertion of (3) into (1) and (2) and with the change of variables $u = \bar{u}$, $v = j\bar{v}$, $p = \bar{p}$, one obtains the following relations:

$$\frac{\partial u}{\partial t} = -\frac{\partial p}{\partial x} + \nu \left( \frac{\partial^2 u}{\partial x^2} - k^2 u \right) \tag{4}$$

$$\frac{\partial v}{\partial t} = kp + \nu \left( \frac{\partial^2 v}{\partial x^2} - k^2 v \right) \tag{5}$$

$$\frac{\partial u}{\partial x} + kv = 0 \tag{6}$$

($\bar{u}$ and $\bar{v}$ are the components of $\bar{\mathbf{v}}$ and $j^2 = -1$).

The boundary conditions are

$$u = v = 0, \quad \text{at } x = \pm 1 \tag{7}$$

The initial fields are specified in Section 4. Any solution of equations (4)–(7) may be expanded in eigenfunctions:

$$u(x,t) = -k \sum_{i=1}^{\infty} f_i(x) g_i(t) \tag{8}$$

$$v(x,t) = \sum_{i=1}^{\infty} f_i'(x) g_i(t) \tag{9}$$

where the functions $f_i(x)$ and $g_i(t)$ are

$$f_i(x) = \frac{\cos \mu_i}{k \cosh k} \cosh kx - \cos \mu_i x \tag{10}$$

$$g_i(t) = \exp(-\sigma_i \nu t) \tag{11}$$

with

$$\mu_i = (\sigma_i - k^2)^{1/2} \tag{12}$$

The eigenfunctions $f_i(x)$ and $g_i(t)$ are obtained by variable separation. The coefficient $\sigma_i$ is the decay-rate associated with the $i$th eigenmode. The theoretical value of $\sigma_i$ is obtained from the equation

$$\mu_i \tan \mu_i + k \tanh k = 0 \tag{13}$$

We will restrict ourselves to the calculation of the first eigenmode which is the dominant mode. For $k = 1$, $\sigma_i \approx (i\pi)^2$, so that higher modes are rapidly damped out. The first mode yields $\sigma_1 = 9{\cdot}313799$.

Four numerical methods will be applied to obtain the solution of equations (4)–(7). The comparison of the theoretical value of $\sigma_1$ will be made with the computed decay-rate $\bar{\sigma}_1$, defined in Section 5.

## 3. NUMERICAL SCHEMES

The numerical methods to be used are all based on a Chebyshev approximation for the spatial discretization of the dependent variables. The velocity components and the pressure are expanded in series of Chebyshev polynomials of first kind, namely,

$$\left.\begin{aligned} u_M &= \sum_{m=0}^{M} u_m(t) T_m(x) \\ v_M &= \sum_{m=0}^{M} v_m(t) T_m(x) \\ p_M &= \sum_{m=0}^{M} p_m(t) T_m(x) \end{aligned}\right\} \tag{14}$$

where $u_m$, $v_m$ and $p_m$ are the corresponding time-dependent Chebyshev modes. The classical projection methods (Galerkin, Tau, Collocation)[2] lead to a system of ordinary differential equations. The time integration will be performed by finite differences for the first three algorithms, whereas the last one will rest upon Chebyshev pseudo-spectral calculation in time[3].

### 3.1. *Explicit pressure calculation*

We will apply to (4)–(7) a splitting scheme using a Poisson equation for the pressure calculation, derived from the incompressibility constraint. Therefore, we consider the scheme:

$$\frac{u^{n+1}-u^n}{\Delta t} = -\frac{\partial p^n}{\partial x} + \nu\left(\frac{\partial^2 u^{n+1}}{\partial x^2} - k^2 u^{n+1}\right), \qquad |x| \leqslant 1 \tag{15}$$

$$\frac{v^{n+1}-v^n}{\Delta t} = kp^n + \nu\left(\frac{\partial^2 v^{n+1}}{\partial x^2} - k^2 v^{n+1}\right), \qquad |x| \leqslant 1 \tag{16}$$

$$\frac{\partial^2 p^n}{\partial x^2} - k^2 p^n = \frac{1}{\Delta t}\left(\frac{\partial u^n}{\partial x} + kv^n\right), \qquad |x| \leqslant 1 \tag{17}$$

$$u^{n+1} = v^{n+1} = 0 \quad \text{at} \quad x = \pm 1 \tag{18}$$

Equation (17) is obtained by taking the divergence of equations (15) and (16) and by imposing that $(\partial u/\partial x + kv)^{n+1}$ vanishes identically. In (15)–(18) the superscript indicates the time level, e.g. $t = n\Delta t$, $\Delta t$ being the time step. The momentum equations (15) and (16) are integrated by the backward Euler scheme which is $O(\Delta t)$. As an explicit forward Euler scheme would be constrained by a severe restriction on the time step, i.e. $\Delta t \leqslant \text{constant}/M^4$, an implicit scheme is chosen because of its stability properties. Second-order accuracy in time is achieved on the viscous terms by Richardson extrapolation. The time marching scheme is accomplished in three stages.

It should be mentioned that in 2-D or 3-D codes, the Richardson extrapolation is only performed on the viscous part of the Navier–Stokes equations. The non-linear terms are very often treated by a second order explicit scheme. Richardson extrapolation yields effectively second order accuracy in contrast with the Crank–Nicolson scheme which does not improve very much the time integration.[4] The first solution is obtained by a time integration from $t$ to $t + \Delta t$ and will be denoted by $\mathbf{v}^+$. Afterwards, the scheme (15)–(18) is performed in two steps of $\Delta t/2$ size, producing a solution $\mathbf{v}^*$. The extrapolation formula:

$$\mathbf{v}^{n+1} = 2\mathbf{v}^* - \mathbf{v}^+ \tag{19}$$

gives the final result at the new time level.

Several boundary conditions are applied to (17):

(a) The inviscid pressure boundary condition

$$\frac{\partial p^n}{\partial x} = 0, \quad \text{at } x = \pm 1 \tag{20}$$

This condition is used in large 2-D or 3-D codes, where splitting schemes work as follows: (i) a new velocity field is computed by considering the non-linear terms, (ii) a Poisson equation is solved for the pressure, (iii) pressure gradients are added to the previous velocity field and, finally, (iv) the viscous terms are included and $\mathbf{v}^{n+1}$ is obtained. For the pressure computation in (ii), equation (20) is correct to $O(\nu\Delta t)$, which is a small error term for large Reynolds number flows.

(b) The tangential viscous pressure condition (Dirichlet condition) (derived from equation (16))

$$p^n = -\frac{\nu}{k}\frac{\partial^2 v^n}{\partial x^2}, \quad \text{at } x = \pm 1 \tag{21}$$

(c) The normal viscous pressure condition (Neumann condition) (derived from equation (15))

$$\frac{\partial p^n}{\partial x} = \nu\frac{\partial^2 u^n}{\partial x^2}, \quad \text{at } x = \pm 1 \tag{22}$$

(d) The modified normal pressure condition

$$\frac{\partial p^n}{\partial x} = -\nu k \frac{\partial v^n}{\partial x}, \quad \text{at } x = \pm 1 \tag{23}$$

Equation (23) is derived from (22) using the continuity equation.

Normal pressure conditions such as (22) and (23) are used in most viscous flow computations. It should be noticed that boundary condition (20) does not respect the physics of the problem. However, equation (20) stabilizes the computation whereas equations (21) and (22) lead to instabilities whatever the value of the time step is.[4]

### 3.2. *Influence matrix method*

The fundamental problem associated with the use of the Poisson equation for the pressure $p$ is that the correct boundary conditions for $p$, which imply incompressibility, are not known *a priori* but determined implicitly by the solution. The influence matrix technique (or, as some call it, Green's function technique) makes it possible to obtain these boundary conditions and to satisfy the continuity equation exactly in the discretized problem. This has been proposed in Reference 5 for the present 1-D problem and in Reference 6 for the general case. The 2-D case is treated in Reference 7 using a Chebyshev polynomial approximation and in Reference 8 with finite differences.

We summarize the method as applied for the present problem. For the time discretization of (1) the implicit scheme:

$$\frac{\mathbf{v}^{n+1} - \mathbf{v}^n}{\Delta t} = -\mathbf{grad}\ p + \theta\nu\Delta\mathbf{v}^{n+1} + (1-\theta)\nu\Delta\mathbf{v}^n \tag{24}$$

with $0{\cdot}5 \leqslant \theta \leqslant 1$ is used (it is sufficient to include only one gradient term which is uniquely determined by equation (24) together with equations (2) and (7)).[1] For very stiff problems the choice of $\theta > 0{\cdot}5$ is essential to provide for the necessary damping of the rapidly decaying solution parts. In the following we drop the superscript $n+1$ for ease of notation.

From equations (4)–(6) the Poisson equation

$$\frac{\partial^2 p}{\partial x^2} - k^2 p = 0 \tag{25}$$

is derived. The basis of the solution method is the fact that the continuity equation may be replaced *equivalently* by the Poisson equation for $p$ *and* the condition $\operatorname{div} \mathbf{v} = 0$ on the boundary.[5,6] From equations (6) and (7), this condition reads

$$\frac{\partial u}{\partial x} = 0, \quad \text{at } x = \pm 1 \tag{26}$$

The pressure $p$ and normal velocity component $u$ are determined by equations (25) and (26) and

$$\frac{\partial^2 u}{\partial x^2} - Bu - (\theta\nu)^{-1}\frac{\partial p}{\partial x} = r \tag{27}$$

$$u = 0 \quad \text{at } x = \pm 1 \tag{28}$$

with $B = k^2 + (\theta\nu\Delta t)^{-1}$ and $r$ contains the terms at the previous time level.

Equations (25)–(28) are solved in three steps as follows. First, we compute a solution $\tilde{p}$, $\tilde{u}$ of equations (25), (27) and (28) with arbitrary (e.g. zero) $\tilde{p}(\pm 1)$. In general, this solution has a non-zero

residual $(\partial\tilde{u}/\partial x)(\pm 1)$. The desired solution $p$, $u$ is written as a linear combination:

$$\begin{aligned} p &= \tilde{p} + \delta_1 p_1 + \delta_2 p_2 \\ u &= \tilde{u} + \delta_1 u_1 + \delta_2 u_2 \end{aligned} \tag{29}$$

where $p_i$, $u_i$ are solutions of the homogeneous differential equations ($r = 0$ in equation (27)) with linear independent boundary values, e.g.

$$\begin{aligned} p_1(+1) &= 1, \quad p_2(+1) = 0 \\ p_1(-1) &= 0, \quad p_2(-1) = 1 \end{aligned} \tag{30}$$

The coefficients $\delta_i$ are determined from equations (26) and (29):

$$\begin{pmatrix} \dfrac{\partial u_1}{\partial x}(+1) & \dfrac{\partial u_2}{\partial x}(+1) \\ \dfrac{\partial u_1}{\partial x}(-1) & \dfrac{\partial u_2}{\partial x}(-1) \end{pmatrix} \begin{pmatrix} \delta_1 \\ \delta_2 \end{pmatrix} = - \begin{pmatrix} \dfrac{\partial \tilde{u}}{\partial x}(+1) \\ \dfrac{\partial \tilde{u}}{\partial x}(-1) \end{pmatrix} \tag{31}$$

It is sufficient to calculate the solutions $p_i$, $u_i$ once before starting time integration and to store only the 'influence matrix' (or its inverse) on the left-hand side of equation (31). The second step in the solution procedure therefore consists of solving the linear $2 \times 2$ equation system (31) which is elementary in the present case (in general a system of order of the number of discrete boundary points is to be solved). Once $\delta_1$ and $\delta_2$ are known, the correct pressure boundary values are available:

$$\begin{aligned} p(+1) &= \tilde{p}(+1) + \delta_1 \\ p(-1) &= \tilde{p}(-1) + \delta_2 \end{aligned} \tag{32}$$

Thus, in the third step, $p$ can be calculated from equations (25) and (32) and thereafter $u$ from equations (27) and (28), and finally $v$ is found. In this way, the solution of each time step is obtained by solving sequentially a set of Helmholtz equations with Dirichlet boundary conditions. These are discretized by the Tau method, where some care must be taken to obtain an exactly divergence-free solution.[5]

### 3.3. *Penalty method*

The pressure is often regarded as a Lagrange multiplier associated with the incompressibility condition. Therefore, the penalty formulation has become very popular in the recent past within the finite element numericists.[9,10] This practice avoids the splitting-up of the Navier–Stokes operator, ensures incompressibility and restates the problem only in terms of the velocity field. The penalty method prescribed the following relation for the pressure:

$$\varepsilon p + \operatorname{div} \mathbf{v} = 0 \tag{33}$$

where $\varepsilon$ is called the penalty parameter ($\varepsilon = 10^{-2} \ldots 10^{-14}$).

Equation (33) may be viewed as an equation of state for the pressure field or a direct extension of the artificial compressibility technique. Inserting equation (33) into equation (1), one obtains

$$\frac{\partial \mathbf{v}}{\partial t} = \frac{1}{\varepsilon} \mathbf{grad} (\operatorname{div} \mathbf{v}) + \nu \Delta \mathbf{v} \tag{34}$$

As a consequence, the problem (4)–(6) is replaced by:

$$\frac{\partial u}{\partial t} = \left(v + \frac{1}{\varepsilon}\right)\frac{\partial^2 u}{\partial x^2} - vk^2 u + \frac{k}{\varepsilon}\frac{\partial v}{\partial x} \tag{35}$$

$$\frac{\partial v}{\partial t} = v\frac{\partial^2 v}{\partial x^2} - k^2\left(v + \frac{1}{\varepsilon}\right)v - \frac{k}{\varepsilon}\frac{\partial u}{\partial x} \tag{36}$$

which is a coupled system of equations. The penalty parameter whose optimal choice turns out to be $\varepsilon = 10^{-7}$ (see References 4 and 9), makes the time integration of equations (35) and (36) very difficult as we are faced now with stiff equations. In order to overcome this difficulty, an unconditionally stable backward Euler scheme is applied to the right-hand sides of (35) and (36). Second order accuracy in time is obtained by Richardson extrapolation (see equation (19)).

### 3.4. *Pseudo-spectral space–time method*

Morchoisne,[3,11] proposed a Chebyshev approximation for both space and time discretizations. The solution of equations (4)–(7) is obtained through a pseudo-spectral iterative technique, which generates a sequence of approximations; the solution is the limit of this sequence:

$$\begin{aligned} &U^0, U^1, \ldots, U^l, \ldots \\ &V^0, V^1, \ldots, V^l, \ldots \\ &P^0, P^1, \ldots, P^l, \ldots \end{aligned} \tag{37}$$

where $l$ denotes the current iteration index. The approximations (37) satisfy initial and boundary conditions on the global space–time domain,

$$\begin{aligned} U^0(x,t) &= u(x,0) \\ V^0(x,t) &= v(x,0) \\ P^0(x,t) &= p(x,0) \end{aligned} \tag{38}$$

Every quantity is changed according to the following relations:

$$\begin{aligned} U^{l+1}(x,t) &= U^l(x,t) + \eta\delta u^l(x,t), \\ V^{l+1}(x,t) &= V^l(x,t) + \eta\delta v^l(x,t), \\ P^{l+1}(x,t) &= P^l(x,t) + \eta\delta p^l(x,t), \end{aligned} \tag{39}$$

where $\eta$ is an under-relaxation coefficient and where the variations $\delta u^l, \delta v^l, \delta p^l$ come from a Newton method and satisfy homogeneous initial and boundary conditions.

The variation quantities at the $l$th iteration are obtained from the following equations:

$$\frac{\partial \delta u^l}{\partial t} = -R_u^l - \frac{\partial \delta p^l}{\partial x} + v\left(\frac{\partial^2 \delta u^l}{\partial x^2} - k^2 \delta u^l\right) \tag{40}$$

$$\frac{\partial \delta v^l}{\partial t} = -R_v^l + k\delta p^l + v\left(\frac{\partial^2 \delta v^l}{\partial x^2} - k^2 \delta v^l\right) \tag{41}$$

$$\frac{\partial \delta u^l}{\partial x} + k\delta v^l = -R_p^l \tag{42}$$

In the right-hand sides of equations (40)–(42), the residues $R_u^l$, $R_v^l$, $R_p^l$ are given by the following

expressions:

$$R_u^l = \frac{\partial U^l}{\partial t} + \frac{\partial P^l}{\partial x} - \nu\left(\frac{\partial^2 U^l}{\partial x^2} - k^2 U^l\right) \tag{43}$$

$$R_v^l = \frac{\partial V^l}{\partial t} - kP^l - \nu\left(\frac{\partial^2 V^l}{\partial x^2} - k^2 V^l\right) \tag{44}$$

$$R_p^l = \frac{\partial U^l}{\partial x} + kV^l \tag{45}$$

Time and space derivatives are computed by using formal derivation of Chebyshev polynomials expansions. All details are given in Reference 11.

Equations (40)–(42) giving velocity–pressure variations, are solved in two steps. First, pressure variations are obtained from a Poisson equation, deduced by taking the divergence of the equations (40) and (41), and using equation (42):

$$\frac{\partial^2 \delta p^l}{\partial x^2} - k^2 \delta p^l = \frac{\partial R_p^l}{\partial t} + \nu\left(k^2 R_p^l - \frac{\partial^2 R_p^l}{\partial x^2}\right) - kR_v^l - \frac{\partial R_u^l}{\partial x} \tag{46}$$

Equation (46) is solved by finite differences with classical Neumann boundary conditions.

$$\frac{\partial \delta p^l}{\partial x} = -R_u^l + \nu\left(\frac{\partial^2 \delta u^{l-1}}{\partial x^2}\right), \quad \text{at } x = \pm 1 \tag{47}$$

As for residues the right-hand side of equation (46) is computed by means of the spectral representation.

Then, the solution of equations (40)–(42) rests upon a centred finite-difference scheme based on the Chebyshev collocation points (in space and time). The time derivatives in equations (40) and (41) are approximated by an implicit Crank–Nicolson scheme.

To reduce the number of harmonics in time discretization, the total time integration domain may be divided into subdomains. The iterative process is performed in each subdomain; the initialization of the next time subdomain is given by the values of velocity and pressure obtained at the end of the previous subdomain.

## 4. CHOICE OF THE INITIAL VELOCITY FIELD

It is usually agreed that the initial velocity field for the Navier–Stokes equations has to satisfy the boundary conditions and to be divergence-free. However these conditions are not sufficient to generate a solution which is regular in the whole space–time domain. For example, for the present 2-D Stokes problem (4)–(7) let us consider the initial velocity field:

$$\mathrm{I}\begin{cases} u_0(x) = -k(1-x^2)^2 & (48) \\ v_0(x) = 4x(x^2-1) & (49) \end{cases}$$

The associated pressure can be obtained from the Poisson equation:

$$\frac{\partial^2 p_0}{\partial x^2} - k^2 p_0 = 0 \tag{50}$$

whose solution is of the form:

$$p_0(x) = C_1 \sinh kx + C_2 \cosh kx \tag{51}$$

The two constants are derived from the imposition of the boundary conditions. The Dirichlet condition (21) yields

$$p_0 = p_{ID} = \frac{-24\nu}{k \sinh k} \sinh kx \tag{52}$$

whereas the Neumann condition (22) leads to

$$p_0 = p_{IN} = \frac{-8\nu}{\cosh k} \sinh kx \tag{53}$$

Obviously we do not have a unique pressure distribution as should be expected for a regular solution. The compatibility condition which the initial velocity field should satisfy to have a regular solution[12] is violated by equations (48) and (49). The condition expresses that the pressure calculated with the Dirichlet condition coincides with the pressure obtained by using the Neumann condition. As a consequence the solution of equations (4)–(7) with initial conditions (48) and (49) will have singularities at the initial instant $t = 0$. From these initial singularities, difficulties with numerical solutions will show up. This will in fact be confirmed by our numerical results.

To generate a compatible initial field, we consider now as initial velocity field the first

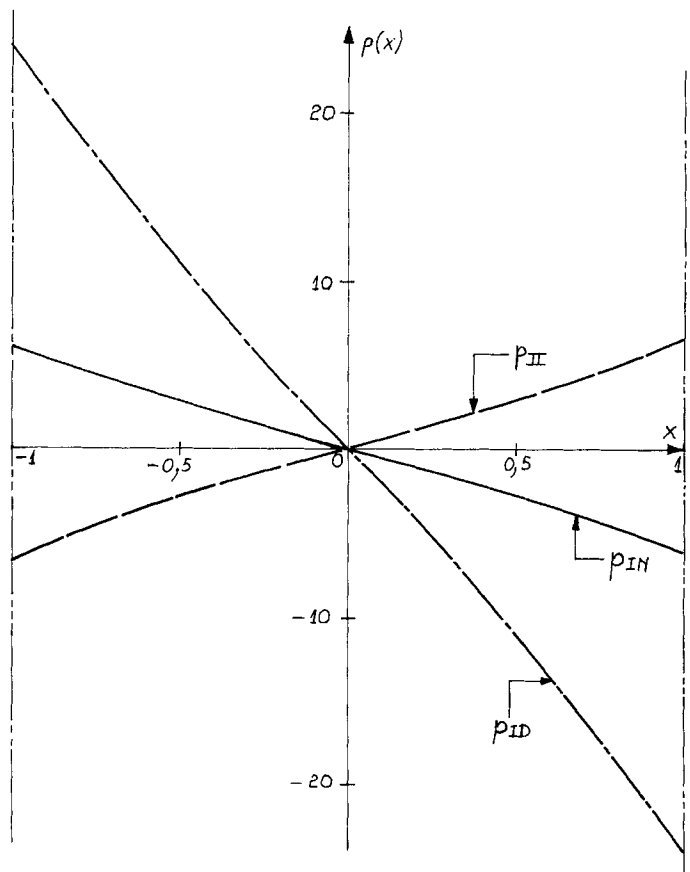


Figure 1. Initial pressure distribution $p_0(x)$: equations (52), (53) and (56)

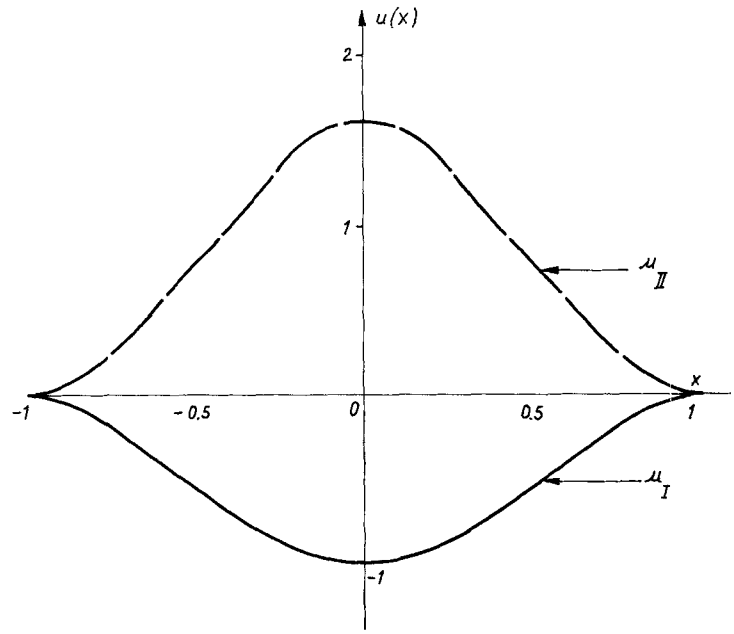


Figure 2. Initial velocity distribution $u_0(x)$: equations (48) and (54)

eigensolution of the Stokes problem (1), (2), namely

$$\text{II}\begin{cases} u_0(x) = -\cos\mu_1 \cosh kx + \cosh k \cos\mu_1 x & (54) \\ v_0(x) = k\cos\mu_1 \sinh kx + \mu_1 \cosh k \sin\mu_1 x & (55) \end{cases}$$

where

$$\mu_1 = (\sigma_1 - k^2)^{1/2}$$

Here, the pressure satisfies both Dirichlet and Neumann conditions and is given by:

$$p_0 = p_{II} = -\nu\sigma_1 \frac{\cos\mu_1}{k\cosh k} \sinh kx \tag{56}$$

Figures 1–3 show the various components of both initial fields on the $|x| \leqslant 1$ range.

For the space–time pseudo-spectral method, it is necessary to provide an initial profile for the pressure field. The Dirichlet pressure (equation (52)) will be systematically used with the first initial field, whereas (56) is used in case II.

## 5. RESULTS

In order to compare the various numerical methods and to examine the influence of the initial conditions and pressure treatment, a computed decay-rate $\bar{\sigma}$ is defined as follows:

$$\bar{\sigma}_{[t,T]} = -\frac{1}{\nu T} \ln \frac{u(x=0, t+T)}{u(x=0, t)} \tag{57}$$

The reference velocity is taken at $x = 0$ as the maximum value is reached at that point (Figure 2). We will choose $T = 1$. In addition to $\bar{\sigma}_{[0,1]}$ which is computed from the actual solution, a

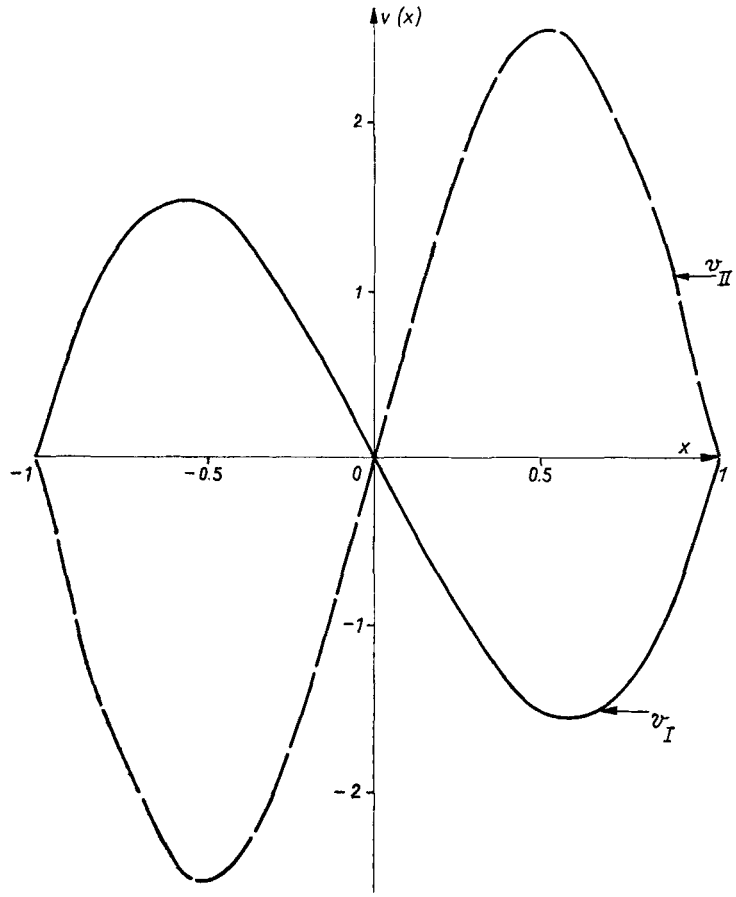


Figure 3. Initial velocity distribution $v_0(x)$: equations (49) and (55)

theoretical decay-rate may be estimated. For the time differencing scheme (24) and for the $i$th eigenmode $g_i(t) = \exp(-\nu\sigma_i\Delta t)$, one gets

$$\bar{\sigma}^i_{\text{pred}} = \frac{-1}{\nu\Delta t} \ln \frac{1-(1-\theta)\nu\sigma_i\Delta t}{1+\theta\nu\sigma_i\Delta t} \tag{58}$$

where $\theta = 0{\cdot}5$ corresponds to the Crank–Nicolson scheme and $\theta = 1$ corresponds to the Euler backward scheme. Therefore, one may easily compute the predicted $\bar{\sigma}$ for the Richardson extrapolation (19).

All the computations are carried out for the first Fourier mode $k = 1$ and a kinematic viscosity $\nu = 1$. With these parameters, the solution decreases by four orders of magnitude in $0 \leqslant t \leqslant 1$. The time step for the first three methods is fixed at $\Delta t = 0{\cdot}01$. The spatial cut-off of the Chebyshev representations (14) is $M = 16$, which is sufficient to achieve spectral accuracy for the space discretization (at least 10 correct decimal places).

An important aspect of time integration is the stiffness of the equations, which becomes more and more serious with increasing Chebyshev cut-off $M$, where rapidly decaying eigenmodes are

excited by the initial distribution (case I). The damping factor according to equation (58),

$$\frac{1-(1-\theta)\nu\sigma_i\Delta t}{1+\theta\nu\sigma_i\Delta t} \tag{59}$$

Table I. Comparison between the computed decay rate and the theoretical value. $\sigma_1 = 9{\cdot}3137399$, $\nu = 1$, $k = 1$, spatial cut-off $M = 16$, time $t = 1$, initial field I

| Explicit pressure calculation Section 3.1 Time step $\Delta t = 10^{-2}$ | Influence matrix Section 3.2 Time step $\Delta t = 10^{-2}$ | Penalty Section 3.3 Time step $\Delta t = 10^{-2}$ | Space–time pseudo-spectral Section 3.4 |
|---|---|---|---|
| B.C. (20) $\bar{\sigma}_{[0,1]} = 9{\cdot}288619$ | $\theta = 0{\cdot}50$, $\bar{\sigma}_{[0,1]} = 9{\cdot}325624$ | $\varepsilon = 10^{-3}$, $\bar{\sigma}_{[0,1]} = 9{\cdot}298721$ | Time monodomain: |
| | $\bar{\sigma}_{\text{pred}} = 9{\cdot}320415$ | | $M_t = 256$ |
| B.C. (21) unstable | | $\varepsilon = 10^{-7}$, $\bar{\sigma}_{[0,1]} = 9{\cdot}301965$ | $\Delta t_{\max} = 0{\cdot}012$ |
| | | | $\bar{\sigma}_{[0,1]} = 9{\cdot}4651$ |
| B.C. (22) unstable | $\theta = 0{\cdot}51$, $\bar{\sigma}_{[0,1]} = 9{\cdot}311270$ | | |
| | $\bar{\sigma}_{\text{pred}} = 9{\cdot}311807$ | $\varepsilon = 10^{-11}$, $\bar{\sigma}_{[0,1]} = 9{\cdot}301926$ | 10 time subdomains |
| B.C. (23) $\bar{\sigma}_{[0,1]} = 9{\cdot}297928$ | | | $M_t = 16$ for each subdom. |
| | $\theta = 0{\cdot}52$, $\bar{\sigma}_{[0,1]} = 9{\cdot}302607$ | | $\bar{\sigma}_{[0,1]} = 9{\cdot}1450$ |
| $\bar{\sigma}_{\text{pred}} = 9{\cdot}301570$ | $\bar{\sigma}_{\text{pred}} = 9{\cdot}303216$ | | |
| | | | 20 time subdomains |
| | $\theta = 0{\cdot}53$, $\bar{\sigma}_{[0,1]} = 9{\cdot}294032$ | $\bar{\sigma}_{\text{pred}} = 9{\cdot}301570$ | $M_t = 8$ for each subdom. |
| | $\bar{\sigma}_{\text{pred}} = 9{\cdot}294641$ | | $\bar{\sigma}_{[0,1]} = 8{\cdot}0121$ |
| B.C.: Boundary condition | Number of subdivisions of the first time integration interval: 10 | | $M_t$: time cut-off Initial pressure: equation (52) |

Table II. Comparison between the computed decay rate and the theoretical value. $\sigma_1 = 9{\cdot}3137399$, $\nu = 1$, $k = 1$, spatial cut-off $M = 16$, time $t = 1$, initial field II

| Explicit pressure calculation Section 3.1 Time step $\Delta t = 10^{-2}$ | Influence matrix Section 3.2 Time step $\Delta t = 10^{-2}$ | Penalty Section 3.3 Time step $\Delta t = 10^{-2}$ | Space–time pseudo-spectral Section 3.4 |
|---|---|---|---|
| B.C. (20) $\bar{\sigma}_{[0,1]} = 9{\cdot}288619$ | $\theta = 0{\cdot}50$, $\bar{\sigma}_{[0,1]} = 9{\cdot}320482$ | $\varepsilon = 10^{-3}$, $\bar{\sigma}_{[0,1]} = 9{\cdot}29872$ | Time monodomain: |
| | $\bar{\sigma}_{\text{pred}} = 9{\cdot}320481$ | | $M_t = 256$ |
| | | $\varepsilon = 10^{-7}$, $\bar{\sigma}_{[0,1]} = 9{\cdot}30196$ | $\Delta t_{\max} = 0{\cdot}012$ |
| B.C. (21) unstable | $\theta = 0{\cdot}51$, $\bar{\sigma}_{[0,1]} = 9{\cdot}311796$ | | $\bar{\sigma}_{[0,1]} = 9{\cdot}3137396$ |
| | $\bar{\sigma}_{\text{pred}} = 9{\cdot}311796$ | $\varepsilon = 10^{-11}$, $\bar{\sigma}_{[0,1]} = 9{\cdot}30192$ | |
| B.C. (22) unstable | | | 10 time subdomains |
| | $\theta = 0{\cdot}52$, $\bar{\sigma}_{[0,1]} = 9{\cdot}303127$ | | $M_t = 16$ for each subdom. |
| B.C. (23) $\bar{\sigma}_{[0,1]} = 9{\cdot}297928$ | $\bar{\sigma}_{\text{pred}} = 9{\cdot}303127$ | | $\bar{\sigma}_{[0,1]} = 9{\cdot}3137398$ |
| | $\theta = 0{\cdot}53$, $\bar{\sigma}_{[0,1]} = 9{\cdot}294474$ | $\bar{\sigma}_{\text{pred}} = 9{\cdot}301570$ | 20 time subdomains |
| $\bar{\sigma}_{\text{pred}} = 9{\cdot}301570$ | $\bar{\sigma}_{\text{pred}} = 9{\cdot}294474$ | | $M_t = 8$ for each subdom. |
| | | | $\bar{\sigma}_{[0,1]} = 9{\cdot}3137398$ |
| B.C. Boundary Condition | No subdivision of the first time integration interval | | $M_t$: time cut-off Initial pressure: equation (56) |

tends to $-(1-\theta)/\theta$ as $v\sigma_i\Delta t$ goes to infinity. For $\theta = 0{\cdot}5$ the damping factor tends to $-1$ so that oscillations occur and the higher modes are not damped. For $\theta = 1$ this factor goes to zero and all the higher modes disappear.

Results are displayed in Table I for the first initial velocity field (I) and in Table II for the second field (II). They will be analysed for each method.

### 5.1. *Explicit pressure calculation*

In this case, the results at $t = 1$ are not sensitive to the initial conditions. The same behaviour is observed for both initial velocity fields. However the accuracy of the time integration depends strongly on the applied boundary conditions for the pressure computation.

The inviscid pressure condition (20) leads to a computed decay-rate which has only one significant digit. This dismal performance is essentially due to an error occurring in a boundary layer induced by imposing a wrong condition.[4] The tangential and normal pressure conditions (21) and (22) are unstable.

Even if the time step is reduced to values of the order of an explicit conditionally stable scheme, i.e $\Delta t \leqslant cM^4$ ($\Delta t \sim 10^{-6}$), the instability arises after several hundreds of time steps and diverges very slowly. The elaboration of an exact Tau method[2] instead of truncating the matrix system for the boundary conditions fulfilment does not help to cure the problem. The fourth case (equation (23)), where the continuity equation has been used, improves the decay-rate to a value of $\bar{\sigma}_{[0,1]} = 9{\cdot}297928$ which should be compared to $\bar{\sigma}_{\text{pred}} = 9{\cdot}301570$. As mentioned earlier, this kind of boundary condition has been extensively applied in the finite difference approximation and appears to be a good choice, when the pressure comes from a Poisson equation.

### 5.2 *Influence matrix method*

The influence matrix method is very well suited to handle the pressure calculation and fulfilment of the continuity equation. This method treats both initial velocity fields comparable well if the stiffness is handled properly. The only appreciable error left in the numerical results seems to be the time-differencing error. This can be seen from the results for case II (Table II) where the numerical $\bar{\sigma}_{[0,1]}$ is indeed in complete agreement with the predicted value (58). Case II presents only time differencing errors and as the velocity field respects both normal and tangential pressure boundary conditions, the spatial discretization induces only negligible error.

To minimize initial time-differencing errors in general applications and to improve the stiffness treatment in case I of the present problem, a reduced time step is used over the first $\Delta t$ interval. This procedure prevents the numerical solution being polluted by earlier time-stepping errors.

For this case (Table I), the Crank–Nicolson scheme ($\theta = 0{\cdot}5$) fails to produce good results when the first time interval is not subdivided. Considerable oscillations in $\bar{\sigma}_{[0,n\Delta t]}$ occur as $n$ goes to 100. Therefore, the first $\Delta t$ is subdivided into 10 subintervals and $\theta$ is taken greater than 0·5. The number of correct decimal places increases with $\theta$, indicating that the higher eigenmodes are sufficiently damped out. One may conclude that the time differencing scheme, equation (24), needs a value for $\theta > 0{\cdot}5$ in order to treat properly the stiffness character of the discretized system.

### 5.3. *Penalty method*

Like the explicit pressure computation, the performance of penalty method is totally independent of the initial velocity field.

Of course, in this case, the choice of the penalty parameter is critical. An exploration of the $\varepsilon$

range between $10^{-2}$ and $10^{-14}$ shows that the optimal choice is $\varepsilon = 10^{-7}$. Lower $\varepsilon$ values ($10^{-10} \ldots 10^{-14}$) induce round-off errors, whereas higher $\varepsilon$ values ($10^{-2} \ldots 10^{-6}$) do not provide excellent computed $\bar{\sigma}_{[0,1]}$ values. The good behaviour of $\varepsilon = 10^{-11}$ in both tables is purely fortuitous.

The time integration of the penalty method calls for a further comment. As the optimal choice of $\varepsilon$ is $10^{-7}$, equations (35) and (36) present very high values for the coefficients of second-order derivatives. This particular behaviour imposes treating the right-hand sides implicitly by the backward Euler-scheme and second-order accuracy in time is only recovered by the Richardson extrapolation.

The extension of this procedure to 2-D and 3-D Chebyshev spectral representation for the full Navier–Stokes equations is not obvious and requires further investigation due to the stiff character of the penalized equations.

### 5.4. *Pseudo-spectral space-time method*

Owing to the excellent accuracy of the time scheme used in this method, the comparison is done between the computed decay rate $\bar{\sigma}_{[0,1]}$ and the theoretical value $\sigma_1$.

In the case of a mono-domain in time, a very large cut-off $M_t = 256$ was chosen to obtain a value for the maximum time-step $\Delta t$ of the same order of magnitude as in the other method. The iterative process is stopped when the maximum values of the variations $\delta u^l, \delta v^l, \delta p^l$ are $\leqslant 10^{-12}$. For the initial field I (Table I), the $\bar{\sigma}_{[0,1]}$ value does not compare favourably with the theoretical value. The iterative process needs an initial pressure field and a computational speed-up is obtained if that pressure field is well chosen. The expression (52) is not a good guess from this point of view. The computation performed with the pressure (53) satisfying the Neumann condition yields a better result $\bar{\sigma}_{[0,1]} = 9{\cdot}3133$. For the second case (Table II) the full pseudo-spectral scheme achieves spectral accuracy. Dirichlet and Neumann conditions are satisfied for the initial pressure field and the solution has sufficient smoothness properties to be approximated with high accuracy by Chebyshev polynomials.

The time domain may be subdivided into smaller subdomains to produce the solution with less computing effort. For example, the use of 10 subdomains each of them with 17 harmonics, cuts the execution time by a factor of two compared to the mono-domain approach.

The multidomain procedure gives however poor results for the initial field I. The $\bar{\sigma}_{[0,1]}$ value is even worse for 20 time subdomains with $M_t = 8$. In each subdomain, the spectral calculation is based on only a few harmonics for a wrong choice of the initial pressure.

For the second field II (Table II), no noticeable difference is observed between 10 and 20 subdomains, and the computed $\bar{\sigma}_{[0,1]}$ is in excellent agreement with the theoretical value.

Additional results for this problem within the framework of this pseudo-spectral space-time method are presented in Reference 13. More initial fields are considered, and the influence of a Chebyshev staggered grid is carefully examined.

### 5.5. *Remark*

The comparison of computing times is quite difficult. The authors worked independently on different computers and used different programming languages. One of us (L.K.) solved this test problem with CHANSON[5,6] 3-D code written in PL/1, which has a large overhead cost for the Stokes problem at hand. Therefore, it was decided to avoid such a comparison, which is meaningless in this context.

## 6. CONCLUSIONS

The numerical results presented here show that the explicit pressure calculation does not give good results. The influence matrix method, penalty and space-time pseudo-spectral algorithms give the best results, taking into account the accuracy of time schemes. Particularly, this pseudo-spectral space–time technique allows us to reach full space and time spectral accuracy and, here, the computed $\bar{\sigma}_{[0,1]}$ agrees with the theoretical value $\sigma_1$.

From the mathematical point of view, the initial velocity field must satisfy the compatibility condition so that the resulting pressure is required to satisfy both Neumann and Dirichlet boundary conditions at every time and therefore also at the initial time $t = 0$. The penalty method does not require such a condition as the incompressibility constraint is slightly relaxed and, furthermore, the problem is reformulated only in terms of velocity components.

If possible the initial velocity field should be elaborated so that no singularity occurs at the initial time. This regularity enforcement is essential for the pseudo-spectral space–time scheme as it is based on a global expansion. However, finite difference schemes in time are also sensitive to this condition as was observed by the influence matrix method process, when applied to the first initial field.

In most applications, however, it will be very difficult to build initial compatible fields. Therefore the numerical algorithm has to be designed in such a way that it has sufficient damping properties to cope with the initial singularities at the very beginning of the time-integration.

## REFERENCES


1. L. Kleiser, *Numerische Simulationen zum laminar-turbulenten Umschlagsprozeß der ebenen Poiseuille-strömung*, Dissertation Karlsruhe, 1982, Kernforschungszentrum Karlsruhe, KFK 3271.
2. D. Gottlieb and S. A. Orszag, *Numerical Analysis of Spectral Methods: Theory and Applications*, SIAM monograph no. 26, Philadelphia, Pennsylvania, 1977.
3. Y. Morchoisne, 'Résolution des équations de Navier–Stokes par une méthode pseudo-spectrale en espace-temps', *La Recherche Aérospatiale*, no. 1979–5, pp. 293–306, (English translation).
4. M. Deville and S. A. Orszag, 'Splitting methods for incompressible problems', Submitted to *Journal of Computational Physics* (1983).
5. L. Kleiser and U. Schumann, 'Treatment of incompressibility and boundary conditions in 3-D numerical spectral simulations of plane channel flows', in Hirschel, E. H. (ed.), *Proc. 3rd GAMM Conference on Numerical Methods in Fluid Mechanics*, Vieweg-Verlag Braunschweig, 1980, pp. 165–173.
6. L. Kleiser and U. Schumann, 'Spectral simulations of the laminar–turbulent transition process in plane Poiseuille flow', *Symposium on Spectral Methods for Partial Differential Equations*, 16–18 August 1982, ICASE, NASA Langley Research Center, Hampton, Va. Proceedings published by SIAM, Philadelphia, Pa. (1984)
7. P. Le Quere and T. Alziary de Roquefort, 'Sur une méthode spectrale semi-implicite pour la résolution des équations de Navier–Stokes d'un écoulement bidimensionnel visqueux incompressible', *C. R. Acad. Sc. Paris*, **294,** Série II, 941–944 (1982).
8. U. Schumann, 'Direct finite difference Stokes solver', *Zamm* **64,** T227–T229 (1984).
9. T. J. R. Hughes, W. K. Liu and A. Brooks, 'Finite element analysis of incompressible viscous flows by the penalty function formulation', *J. Comp. Phys.*, **30,** 1–60 (1979).
10. J. N. Reddy (Ed.), *'Penalty-Finite Element Methods in Mechanics'*, Applied Mechanics Division, Vol. 51, ASME Publication 1982.
11. Y. Morchoisne, 'Inhomogeneous flow calculations by spectral methods: monodomain and multidomain technique', *Symposium on Spectral Methods for Partial Differential Equations*, 16–18 August 1982, ICASE, NASA Langley Research Center, Hampton, Va. Proceedings published by SIAM, Philadelphia, Pa. (1984).
12. J. G. Heywood and R. Rannacher, 'Finite-element approximation of the non-stationary Navier–Stokes problem (I)', *SIAM Journal of Numerical Analysis*, **19,** 275–311 (1982).
13. F. Monitigny-Rannou, 'Influence of compatibility conditions in numerical simulation of inhomogeneous incompressible flows' Pandolfi M-Piva R (Eds). *Proc. 5th. GAMM Conference on Numerical Methods in Fluid Mechanics*, Vieweg-Verlag, Braunschweig, 1984, pp. 234–242.